metals

MDPI

Article

Viscosity Estimation of TiO_2-Bearing Blast Furnace Slag with High Al_2O_3 at 1500 °C

Haiyan Zheng [1,2,*], Shifa Zhou [3], Shen Zhang [1,2], Yang Li [4], Baozhi Zhang [1,2,5], Fengman Shen [1,2], Zhonghua Wang [4] and Tao Han [4]

1 Key Laboratory for Ecological Metallurgy of Multimetallic Mineral (Ministry of Education), Northeastern University, Shenyang 110819, China
2 School of Metallurgy, Northeastern University, Shenyang 110819, China
3 Iron and Steel Company, WISDRI Engineering and Research Incorporation Limited, Wuhan 430080, China
4 Xuanhua Iron and Steel Group Co., Ltd., Hebei Iron & Steel Group Co. Ltp, Xuanhua 075100, China
5 Beris Engineering and Research Corporationuanhua, Qingdao 266000, China
* Correspondence: zhenghy@smm.neu.edu.cn

Abstract: Slag compositions are significant for the viscosity of blast furnace slag. An improved Urbain model (IUM) was proposed by introducing R_5 ($(X(CaO) + X(MgO) + 2X(TiO_2))/(2X(SiO_2) + 3X(Al_2O_3))$) and N ($X(MgO)/3X(Al_2O_3)$) as the model parameters. By comparing IUM with other models, the model parameters of R_5 and N are more reasonable and suitable for TiO_2-bearing blast furnace slag, and IUM for predicting viscosity has a higher precision, and its relative error is only 10%. The viscosity isolines of the CaO–SiO_2–15%Al_2O_3–MgO–2.5% TiO_2 system were plotted, and the results show that the viscosity center of the slag is between R_{w2} ($w(CaO)/w(SiO_2)$) = 0.77–1.39 and N_w ($w(MgO)/w(Al_2O_3)$) = 0–1.37, the value of the viscosity center is 0.3 Pa·s, the viscosity increases gradually from the center to the outside, and the viscosity of the slag gradually decreases with the increase in N_w and R_{w2}. Furthermore, FTIR (Fourier Transform Infrared Spectroscopy) analysis was carried out in order to understand the mechanism between the slag structure and viscosity. With the increase in N_w and R_{w2}, the peak values of the symmetrical stretching vibration of non-bridging oxygen in the Si–O tetrahedral structure of slag decrease, and the slag structures depolymerize, which leads to the decrease in the viscosity of the slag.

Keywords: TiO_2-bearing blast furnace slag; viscosity estimation; improved Urbain model (IUM); viscosity isoline; FTIR analysis

Citation: Zheng, H.; Zhou, S.; Zhang, S.; Li, Y.; Zhang, B.; Shen, F.; Wang, Z.; Han, T. Viscosity Estimation of TiO_2-Bearing Blast Furnace Slag with High Al_2O_3 at 1500 °C. *Metals* **2023**, *13*, 573. https://doi.org/10.3390/met13030573

Academic Editor: Ricardo J. Alves de Sousa

Received: 5 February 2023
Revised: 10 March 2023
Accepted: 11 March 2023
Published: 13 March 2023

1. Introduction

In the process of blast furnace (BF) ironmaking, the viscosity of blast furnace slag plays an important role in blast furnace smelting, so it is very meaningful to investigate the relationship of viscosity with slag composition [1,2]. In recent years, many iron and steel enterprises have had to adopt oversea ores (from Australia), with the lack of high-grade ores in China, in order to reduce the production cost. The main difference between Australian ore and Chinese ore is that the content of Al_2O_3 in Australian ore is higher, so the usage of Australian ore in large amounts will inevitably lead to an increase in the Al_2O_3 content in the slag. In addition, the erosion of the blast furnace body is deteriorated due to the increase in smelting strength, and the quality of the hearth and bottom of the furnace has become the main factor affecting the life of the first generation of blast furnaces [3,4]. In order to protect the hearth and bottom of the furnace, alkaline low titanium slag is often used, and this leads to a small amount of TiO_2 in the slag [5]. Based on the abovementioned background, it is significant to investigate the effects of the composition of slag on the viscosity.

At present, the method for measuring the viscosity of blast furnace slag is commonly conducted by the rotating column method in a laboratory. Although this method can obtain the viscosity of BF slag accurately, it takes time and effort, along with a high economic cost.

Therefore, developing a viscosity prediction model of slag containing TiO_2 and high Al_2O_3 not only obtains the viscosity of blast furnace slag efficiently but also saves time spent on viscosity measurement and reduces the cost. The traditional idea is that the content of Al_2O_3 is more than 16%, which is very bad for blast furnace smelting.

The existing viscosity prediction models mainly include an empirical model and a structural model. The empirical model is based on a large number of viscosity experimental data to optimize the model and obtain the empirical equation to improve the accuracy of the model, and the model is mainly divided into the Urbain model [6], modified Urbain model [7–10], NPL model [11], Zhao model [12], etc. The structure model is mainly based on the slag structure, takes into account the deep internal structure of silicate melt, and includes the KTH model [13], Iida model [14], and Zhang model [15]. The structural model is characterized by the relationship between the slag viscosity and deep internal structure, so the calculation is relatively cumbersome and usually needs to be carried out with the help of specific software. Compared with other models [16–18], the Urbain model is simple and belongs to the empirical model, whose accuracy can be improved by using a large amount of data fitting. Previous research shows that the improved Urbain model (IUM) is suitable for the $CaO–SiO_2–Al_2O_3–MgO$ quaternary slag system by modifying the Urbain model parameters [19], and its relative error is 24%, which is better than that of most of the models. Therefore, an improved Urbain model (IUM) for $CaO–SiO_2–Al_2O_3–MgO–TiO_2$ is proposed by introducing two of the modified model parameters, R_5 ($(X(CaO) + X(MgO) + 2X(TiO_2))/(2X(SiO_2) + 3X(Al_2O_3))$) and N ($X(MgO)/3X(Al_2O_3)$), for predicting the viscosity of the slag in this paper. In addition, the effect of slag structure on viscosity was also explored.

2. Improved Urbain Model (IUM Model)

2.1. Definition of the Model Parameters

The Urbain model is based on the theory of liquid dynamics, and its basic equation is the Weymann-Frenkel equation.

$$\eta = ATexp^{\frac{1000B}{T}} \tag{1}$$

where η is the viscosity (poise), A is the pre-exponential factor (poise/K), T is the absolute temperature (K), B is the viscous activation energy (J/mol), and A and B are functions of slag composition.

Taking logarithms on both sides of the Weymann-Frenkel equation, Equation (2) is obtained as follows:

$$\ln \frac{\eta}{T} = \ln A + \frac{1000}{T} B \tag{2}$$

In metallurgical production, the weight ratio of main basic oxides to acid oxides in slags is often expressed by either R_{w2} (the weight ratio of $w(CaO)/w(SiO_2)$) or R_w (the weight ratio of (Σw(basic oxide)/Σw(acid oxide)). Presently, N_w (the weight ratio of $w(MgO)/w(Al_2O_3)$) has been gaining more attention due to the increasing use of iron ores with high Al_2O_3 content in recent years [17–19]. Therefore, an improved Urbain model (IUM) is proposed by introducing two of the model parameters, R_5 and N, denoted, respectively, as Equations (3) and (4), which are more reasonable and suitable than not only the original model parameters (X = the mole fraction sum of acid oxide and α = the ratio of the mole fraction sum of basic oxide to the mole fraction sums of basic oxide and amphoteric oxide) in the Urbain model but also R_2 (the ratio of $X(CaO)/(2X(SiO_2))$) and N, because R and N are significant for the metallurgical slag, and the two model parameters of R_5 and N should be dependent on each other, but R_2 is independent of N. In this paper, w in R_w, R_{wi}, and N_w is the weight percent of the composition in the slag, and i in R_{wi} and R_i is the number of slag compositions used in the parameters.

$$R_5 = \frac{X(CaO)+X(MgO)+2X(TiO_2)}{2X(SiO_2)+3X(Al_2O_3)} \tag{3}$$

$$N = \frac{X(\mathrm{MgO})}{3X(\mathrm{Al_2O_3})} \tag{4}$$

where R_5 is denoted as five components' basicity: CaO, MgO, TiO_2, SiO_2, and Al_2O_3, N is the mole ratio of MgO to Al_2O_3, and $X(i)$ is the mole fraction of component i, such as CaO, MgO, Al_2O_3, SiO_2, and TiO_2.

The viscous activation energy B can be expressed as follows:

$$B = B_0 + B_1 R_5 + B_2 {R_5}^2 + B_3 {R_5}^3 \tag{5}$$

$$B_i = a_i + b_i N + c_i N^2 (i = 0,\ 1,\ 2,\ 3) \tag{6}$$

where B_i, a_i, b_i, and c_i are parameters of the model.

According to Equations (5) and (6), the expression of viscous activation energy B can be obtained as Equation (7).

$$\begin{aligned} B = \quad & a_0 + b_0 \times N + c_0 \times N^2 + \left(a_1 + b_1 \times N + c_1 \times N^2\right) \times R_5 \\ & + \left(a_2 + b_2 \times N + c_2 \times N^2\right) \times {R_5}^2 + (a_3 + b_3 \times N + c_3 \times N^2) \times {R_5}^3 \end{aligned} \tag{7}$$

The flow sheet for establishing the model is shown in Figure 1. The major steps in the flow sheet include: (1) Determining m $(1000/T)$ and n $(\ln((\eta \times 10)/T))$; (2) Determining B (A) by using the least square method with MATLAB R2014a software; (3) Model validation by model error analysis for model optimization. Mills et al. [20] said that the model can be considered as high reliability when the relative error (Δ) of the model is less than 35%. Thus, $\Delta < 35\%$ was set as the decision condition for modeling, as shown in Figure 1, i.e., the database and representation data used for the model will be updated until $\Delta < 35\%$.

R_5 indicates that TiO_2 plays a basic oxide role in the all kinds of TiO_2-bearing blast furnace slag with high Al_2O_3. Zhang et al. [21] used molecular dynamics simulation and FTIR (Fourier Transform Infrared Spectroscopy) spectroscopy to study the effect of the change in the ratio of CaO/TiO_2 on the structure of the $CaO–SiO_2–15\%Al_2O_3–MgO–TiO_2$ quinary slag system at 1500 °C. The results showed that the substitution of CaO by TiO_2 could only lead to a slight change in the degree of polymerization, indicating that TiO_2 has similar effects to CaO and that TiO_2 is a basic oxide.

2.2. Determination of m and n

A total of 57 groups of different viscosity data [22–24] were selected, as shown in Table 1. The pre-exponential factor A and viscous activation energy B, corresponding to each group of viscosity data, can be obtained by fitting ln $((\eta \times 10)/T)$ and $1000/T$ linearly. Taking a group of data (1# in Table 1) as an example, ln $((\eta \times 10)/T)$ and $1000/T$ are fitted linearly. The results are shown in Figure 2. As seen in Figure 2, the fitting degree is high (to 0.9988), which indicates that there is a good linear relationship between ln $((\eta \times 10)/T)$ and $1000/T$.

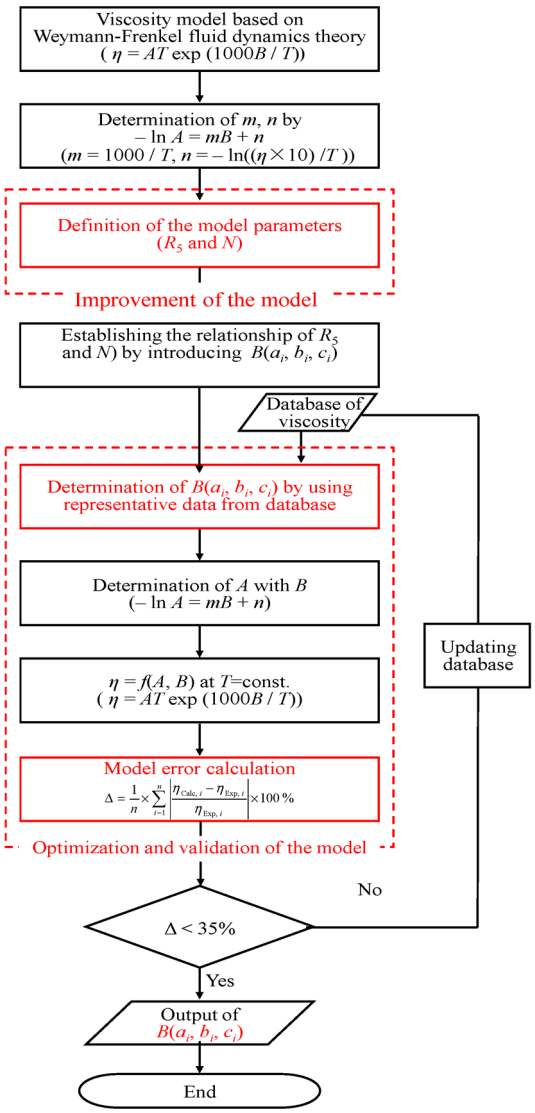

Figure 1. Flow sheet for establishing the model.

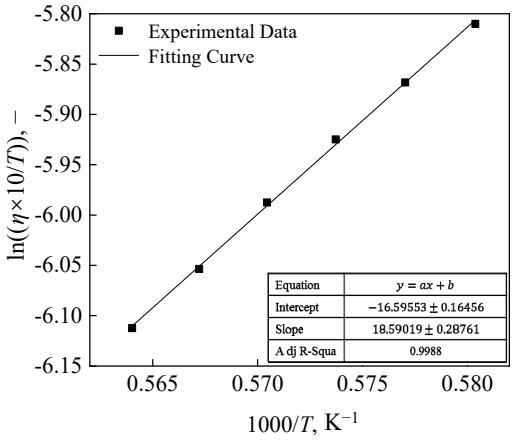

Figure 2. Relationship between viscosity and temperature.

Table 1. Viscosity data used in this study.

No	Chemical Compositions, Mass%					Measured Viscosity, Pa·s *	
	CaO	SiO_2	MgO	Al_2O_3	TiO_2	1450 °C	1500 °C
1# **	42.23	36.72	5.85	13.00	2.20	0.516	0.393
2#	40.68	35.37	6.75	15.00	2.20	0.538	0.409
3#	39.13	34.02	7.65	17.00	2.20	0.556	0.437
4#	41.88	36.42	6.50	13.00	2.20	0.475	0.309
5#	40.28	35.02	7.50	15.00	2.20	0.492	0.346
6#	38.67	33.63	8.50	17.00	2.20	0.528	0.389
7#	41.53	36.12	7.15	13.00	2.20	0.489	0.334
8#	39.88	34.67	8.25	15.00	2.20	0.453	0.335
9#	38.22	33.23	9.35	17.00	2.20	0.485	0.363
10#	43.06	35.89	5.85	13.00	2.20	0.484	0.339
11#	41.48	34.57	6.75	15.00	2.20	0.513	0.351
12#	39.90	33.25	7.65	17.00	2.20	0.530	0.372
13#	42.71	35.59	6.50	13.00	2.20	0.456	0.320
14#	41.07	34.23	7.50	15.00	2.20	0.447	0.311
15#	39.44	32.86	8.50	17.00	2.20	0.489	0.362
16#	42.35	35.30	7.15	13.00	2.20	0.412	0.287
17#	40.66	33.89	8.25	15.00	2.20	0.440	0.316
18#	38.97	32.48	9.35	17.00	2.20	0.421	0.294
19#	43.86	35.09	5.85	13.00	2.20	0.425	0.300
20#	42.25	33.80	6.75	15.00	2.20	0.441	0.331
21#	40.64	32.51	7.65	17.00	2.20	0.488	0.339
22#	43.50	34.80	6.50	13.00	2.20	0.380	0.275
23#	41.83	33.47	7.50	15.00	2.20	0.410	0.317
24#	40.17	32.13	8.50	17.00	2.20	0.439	0.326
25#	43.14	34.51	7.15	13.00	2.20	0.319	0.220
26#	41.42	33.13	8.25	15.00	2.20	0.347	0.248
27#	39.69	31.76	9.35	17.00	2.20	0.380	0.273
28#	41.25	35.25	8.50	14.00	1.00	0.435	0.284
29#	40.92	34.98	8.50	14.00	1.60	0.320	0.242
30#	40.60	34.70	8.50	14.00	2.20	0.308	0.246
31#	39.90	34.10	8.50	16.50	1.00	0.422	0.283
32#	39.58	33.82	8.50	16.50	1.60	0.327	0.25
33#	39.25	33.55	8.50	16.50	2.20	0.321	0.245
34#	39.25	33.55	8.50	16.50	2.20	0.321	0.245
35#	38.71	33.09	9.50	16.50	2.20	0.34	0.218
36#	38.17	32.63	10.50	16.50	2.20	0.327	0.202
37#	35.08	36.92	8.00	19.00	1.00	0.57	0.37
38#	36.88	35.12	8.00	19.00	1.00	0.54	0.35
39#	34.10	35.90	10.00	19.00	1.00	0.61	0.39
40#	35.85	34.15	10.00	19.00	1.00	0.59	0.38
41#	32.15	33.85	8.00	25.00	1.00	0.57	0.36
42#	33.80	32.20	8.00	25.00	1.00	0.55	0.34
43#	31.18	32.82	10.00	25.00	1.00	0.59	0.38
44#	32.78	31.22	10.00	25.00	1.00	0.57	0.36
45#	34.59	36.41	8.00	19.00	2.00	0.53	0.33
46#	36.37	34.63	8.00	19.00	2.00	0.53	0.32
47#	33.62	35.38	10.00	19.00	2.00	0.57	0.35
48#	35.34	33.66	10.00	19.00	2.00	0.55	0.33
49#	31.67	33.33	8.00	25.00	2.00	0.52	0.32
50#	33.29	31.71	8.00	25.00	2.00	0.51	0.3
51#	30.69	32.31	10.00	25.00	2.00	0.56	0.37
52#	32.27	30.73	10.00	25.00	2.00	0.57	0.35
53#	29.20	38.30	2.42	27.80	1.71	1.51	0.98
54#	34.50	35.40	2.11	25.80	1.86	0.94	0.63
55#	38.00	32.00	2.14	25.20	2.28	0.61	0.41
56#	32.00	37.80	4.70	23.30	1.82	0.85	0.57
57#	39.40	32.00	4.80	21.20	2.17	0.41	0.29

*: Nos. 1–27: Experimental data measured by our research group; Nos. 28–57: Experimental data from the literature [22–24]. **: Viscosity is 0.49, 0.47, 0.44, and 0.41 at 1460 °C, 1470 °C, 1480 °C, and 1490 °C, respectively.

The function relationship between the pre-exponential factor A and viscous activation energy B can be determined by linear fitting the obtained pre-exponential factor A and viscous activation energy B, which were obtained from 27 groups of viscosity data in Table 1, and the others were used for model validation. The fitting results are shown in Figure 3. It can be seen in Figure 3 that there is a linear relationship between $-\ln A$ and B,

the fitting degree is as high as 0.99192, and the relationship between the pre-exponential factor A and viscous activation energy B can be obtained, as shown in Equation (8).

$$-\ln A = 0.59B + 5.65 \quad (8)$$

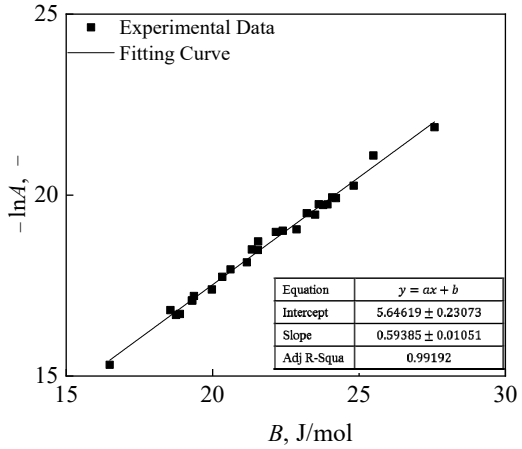

Figure 3. The functional relationship between A and B.

The calculated data of this model are close to those of Zhao's model [12] (0.501 and 7.681) and different from those of the original Urbain model [6] (0.29 and 11.57).

2.3. Determination of Viscous Activation Energy B

According to Equation (7), the viscous activation energy B can be calculated. Because there are 12 unknown parameters (a_i, b_i, c_i) in Equation (7), 12 independent equations (12 groups of viscosity data) are needed to solve the equation. In order to reduce the prediction error of the model, 57 equations are constructed by using 57 groups of viscosity data. The equations are solved by using the least square method with MATLAB software. The solution results of 12 unknown parameters of the model are shown in Table 2.

Table 2. Parameters in Equation (7).

i	a_i	b_i	c_i
0	265.57	−5846.71	−3353.78
1	−1202.13	38,717.73	565.08
2	1480.97	−78,892.50	26,151.32
3	−129.95	50,232.33	−28,517.60

Based on the data in Table 2, the functional relationship between the viscous activation energy B and model parameters (slag composition) can be obtained; Equation (7) can be rearranged, as shown in Equation (9).

$$\begin{aligned} B = \; & 265.5775 - 5846.71 \times N - 3353.78 \times N^2 \\ & + \left(-1202.13 + 38717.73 \times N + 565.0804 \times N^2\right) \times R_5 \\ & + \left(1480.97 - 78892.5 \times N + 26151.32 \times N^2\right) \times {R_5}^2 \\ & + \left(-129.951 + 50232.33 \times N - 28517.6 \times N^2\right) \times {R_5}^3 \end{aligned} \quad (9)$$

For the slag with a given composition, R_5 and N are known. Combined with Equations (8) and (9), the pre-exponential factor A and viscous activation energy B of the slag with a different composition are obtained. Therefore, the viscosity of the slag can be predicted by Equation (1), using B and A obtained from Equations (8) and (9).

2.4. Model Validation

For the titanium-bearing blast furnace slag system, the comparison between the predicted viscosity and the measured viscosity is shown in Figure 4. It can be seen in Figure 4 that the viscosity predicted by IUM is in good agreement with the measured viscosity.

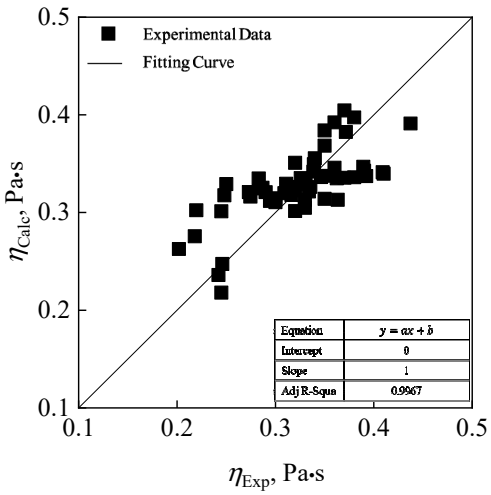

Figure 4. Comparison of predicted viscosity and measured viscosity.

In order to understand the reliability of the model, the relative error (Δ) of the model is determined by Equation (10), and the quantitative calculation is carried out.

$$\Delta = \frac{1}{n} \times \sum_{i=1}^{n} \left| \frac{\eta_{Calc,i} - \eta_{Exp,i}}{\eta_{Exp,i}} \right| \times 100\% \quad (10)$$

where n is the number of data, η_{Calc} is the predicted viscosity, and η_{Exp} is the measured viscosity.

By combining Equations (1), (8), and (9), the viscosity of the slag can be predicted, and the Δ of IUM using Equation (10) is about 10% and far less than 35% of the decision condition, as shown in Figure 1. Thus, it is considered that the prediction effect of IUM is good and that IUM is reliable and of high accuracy.

3. Results and Discussion

3.1. Viscosity Isoline of the CaO–SiO_2–15%Al_2O_3–MgO–2.5%TiO_2 Slag System at 1500 °C

It is well known that slag viscosity plays an important role in blast furnace smelting. Therefore, the viscosity isolines of the CaO–SiO_2–15%Al_2O_3–MgO–2.5%TiO_2 slag system at 1500 °C were plotted based on the calculation data obtained from IUM, and the results are shown in Figure 5. It can be seen in Figure 5 that the center viscosity calculated by IUM is 0.3 Pa·s, and its composition range is between R_{w2} = 0.77–1.39 and N_w = 0–1.37. The viscosity isolines diffuse, and the viscosity increases from the center to the outside gradually. Figure 5 also shows that the viscosity is between 0.3 and 0.4 Pa·s when N_w is 0.45–0.55 and R_{w2} = 1.15–1.25 (the shaded area in Figure 5), in which the slag composition conforms to the practical slag composition for blast furnace smelting. Thus, it shows that the viscosity isoline based on IUM is accurate and that IUM is reliable and will play a certain guiding role in optimizing the slag system for blast furnace smelting.

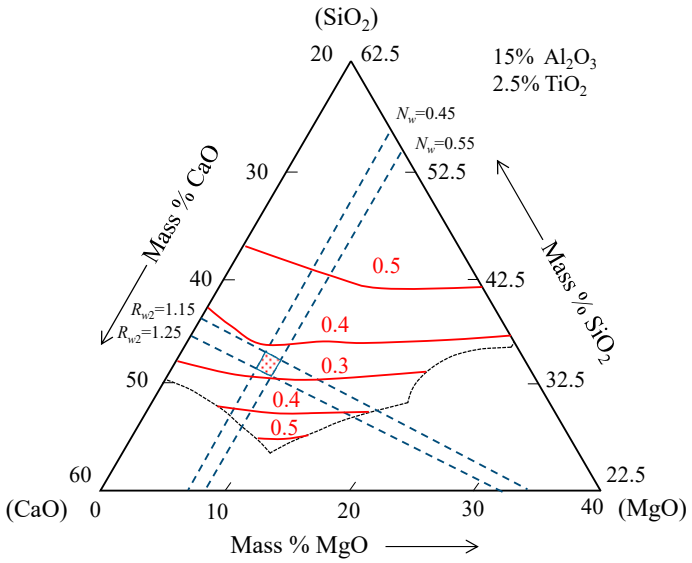

Figure 5. Viscosity isoline of the CaO–SiO_2–15%Al_2O_3–MgO–2.5%TiO_2 slag system at 1500 °C.

3.2. Effect of R_{w2} and N_w on Viscosity

In the process of establishing the model, the model parameters (R_5 and N) are defined with the mole fraction of each component, while the mass fraction is commonly used to express the composition of the slag in the practical production process. Therefore, the influences of R_{w2} (the ratio of w(CaO)/w(SiO_2)) and N_w (the ratio of w(MgO)/w(Al_2O_3)), instead of R_5 and N, on slag viscosity are discussed according to the data obtained from IUM.

According to IUM, the viscosity of slag for a given composition at different temperatures can be calculated. When w(Al_2O_3) is 15% and w(TiO_2) is 2.2%, the viscosity under different R_{w2} and N_w conditions is calculated, and the influences of R_{w2} and N_w on slag viscosity are investigated, respectively. The results are shown in Figure 6.

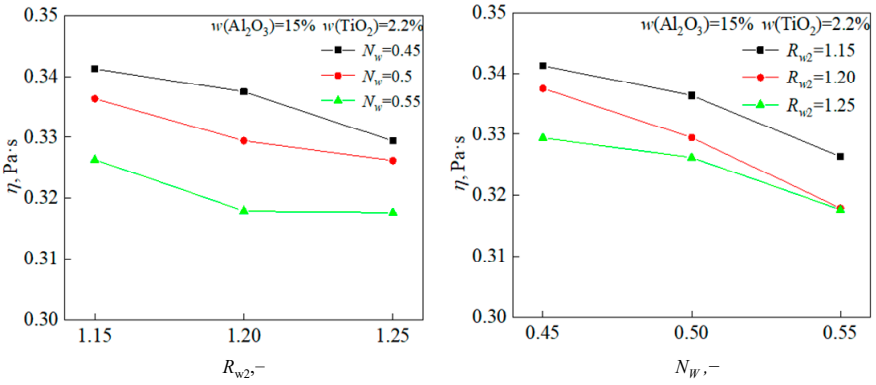

(**a**) Effect of R_{w2} on viscosity (**b**) Effect of Nw on viscosity

Figure 6. Effect of compositions on viscosity at 1500 °C.

It can be seen in Figure 6a that the slag viscosity presents a downward trend when R_{w2} increases. It is considered that the absolute content of CaO in the slag increases with the increase in R_{w2}, CaO provides more (O^{2-}) into the slag, which leads to the depolymerization of the complex silicate and aluminate compounds in the slag, simple structure compounds increase, and viscosity decreases. Figure 6b shows that the slag viscosity gradually decreases with the increase in N_w. Similar to the principle of increasing R_{w2}, the increase in N_w means there is more MgO in the slag, which is a basic oxide, can provide (O^{2-}), and leads to the depolymerization of complex compounds and the decrease in the viscosity of the slag. As a summary, the calculated data obtained from IUM show

that, with the increase in R_{w2} and N_w, the slag viscosity gradually decreases, which is consistent with the change trend of the experimental data.

3.3. Effect of Slag Structure on Viscosity

In order to clear the effect of the slag structure on the viscosity, the slag quenched at 1500 °C was subjected to XRD analysis (X-ray Diffraction Spectroscopy, ultima IV, Rigaku, Japan) with Cu–K_α, at five degrees per minute. The XRD pattern is shown in Figure 7. However, there is no characteristic peak in the XRD pattern of the quenched slag, which indicates that the slag structure is amorphous and complex, and the slag maintains the glassy structure of elevated temperature during the quenching process. Therefore, in order to explore the influence of the slag structure on viscosity, the quenched amorphous slag samples were analyzed by FTIR (Nicolet iS10, Thermo Fisher Scientific, Shanghai, China).

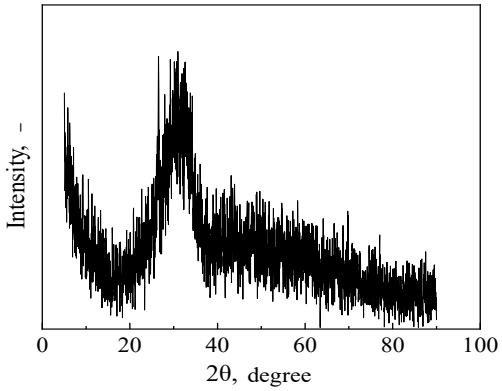

Figure 7. XRD pattern of the quenched slag (Sample 17#).

The FTIR spectrums of the quenched amorphous slag are shown in Figure 8. Generally, the spectrum peak in the range of 800–1200 cm^{-1} represents the symmetric stretching vibration of non-bridged oxygen in the Si–O tetrahedral structure, while the spectrum peak in the range of 400–600 cm^{-1} represents the Al–O tetrahedral structure [25,26]. It can be seen in Figure 8 that the peak values in the range of 800–1200 cm^{-1} and 400–600 cm^{-1} gradually decrease with the increase in R_{w2} (Figure 8a) and N_w (Figure 8b), and this means that the peak values (trough depth) of symmetric stretching vibration of bridging oxygen in Si–O and Al–O tetrahedral structures decrease (i.e., (O^{2-}) increase); the complex Si–O and Al–O tetrahedral structures in the slag were depolymerized into simple compounds, and the viscosity decreased. Therefore, the influence of the slag structure on the viscosity of the slag is due to the change in the composition of the slag.

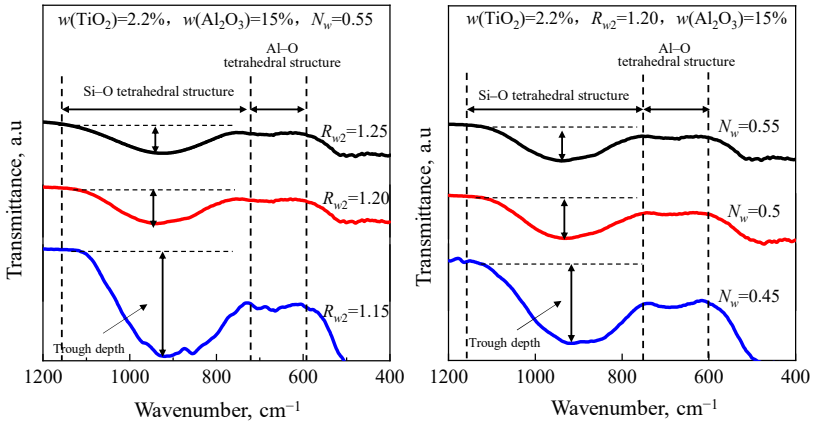

(**a**) Effect of R_{w2} on the slag structure (**b**) Effect of N_w on the slag structure

Figure 8. Effect of the compositions on the slag structure by FTIR.

4. Conclusions

In this paper, an improved Urbain model (IUM) for CaO–SiO_2–Al_2O_3–MgO–TiO_2 was proposed by introducing two of the modified model parameters, R_5 ($(X(CaO) + X(MgO) + 2X(TiO_2))/(2X(SiO_2) + 3X(Al_2O_3))$) and N ($X(MgO)/3X(Al_2O_3)$). Based on IUM, the viscosity isolines were plotted, and the effects of the slag structure on the viscosity were discussed. The main achievements are summarized as follows.

(1) The relative error of IUM is 10%, and this shows that IUM is reliable and is of high accuracy.
(2) The viscosity isolines of the CaO–SiO_2–15%Al_2O_3–MgO–2.5%TiO_2 melts were plotted using the data obtained from IUM. The viscosity center of the slag was located between R_{w2} = 0.77–1.39 and N_w = 0–1.37, and the viscosity value was 0.3 Pa·s, which gradually increased from the center to the outside.
(3) With the increase in N_w and R_{w2}, the peak values of symmetric stretching vibration of bridging oxygen in the Si–O tetrahedral structure decreased, the complex Si–O tetrahedron and Al–O tetrahedron in the slag were depolymerized into simple compounds, and the viscosity of the slag decreased.

Author Contributions: Conceptualization, Methodology, Validation, Formal analysis, Investigation, Project administration, Funding acquisition: H.Z.; Formal analysis, Investigation, Writing—review & editing: S.Z. (Shifa Zhou); Formal analysis, Writing-review & editing: S.Z. (Shen Zhang); Data curation, Formal analysis, Investigation: Y.L.; Formal analysis, Writing—review & editing: B.Z.; Resources, Supervision, Project administration: F.S.; Formal analysis: Z.W.; Investigation: T.H. All authors have read and agreed to the published version of the manuscript.

Funding: This research was funded by the Projects of the National Natural Science Foundation of China (NSFC52074072, NSFC51774071, NSFC51974073, NSFC52074074, and NSFC52074086).

Data Availability Statement: Not applicable.

Conflicts of Interest: The authors declare no conflict of interest.

References

1. Pang, Z.D.; Lv, X.W.; Jiang, Y.Y.; Wei, L.J.; Yan, Z.M. Blast furnace ironmaking process with super-high TiO_2 in the slag: Viscosity and melting properties of the slag. *Metall. Mater. Trans. B* **2020**, *51*, 722–731. [CrossRef]
2. Hu, K.; Tang, K.; Lv, X.W.; Safarian, J.; Yan, Z.M.; Song, B. Modeling viscosity of high titania slag. *Metall. Mater. Trans. B* **2020**, *52*, 245–254. [CrossRef]
3. Zhang, S.R. Prospect of long campaign life technology for blast furnace. *Res. Iron Steel* **2009**, *37*, 1–3.
4. Zou, Z.P.; Xiang, Z.Y.; Ouyang, B.; Wang, L. Design philosophy and countermeasures for long campaign life of blast furnace hearth. *Res. Iron Steel* **2011**, *39*, 38–42.
5. Guo, H.C. Brief discussion on furnace protection technology with titanium-containing materials. *Hunan Metallurgy* **1995**, *23*, 33–37.
6. Urbain, G. Viscosity estimation of slags. *Steel Res. Int.* **1987**, *58*, 111–116. [CrossRef]
7. Riboud, P.V.; Roux, Y.; Lucas, L.D. Improvement of continuous casting powders. *Fachber Huttenprax* **1981**, *290*, 137–140.
8. Kondratiev, A.; Jak, E. Review of experimental data and modeling of the viscosities of fully liquid slags in the Al_2O_3–CaO–'FeO'–SiO_2 system. *Metall. Mater. Trans. B* **2001**, *32*, 1015–1025. [CrossRef]
9. Forsbacka, L.; Holappa, L.; Kondratiev, A.; Jak, E. Experimental study and modelling of viscosity of chromium containing slags. *Steel Res. Int.* **2007**, *78*, 676–684. [CrossRef]
10. Ray, H.S.; Pal, S. Simple method for theoretical estimation of viscosity of oxide melts using optical basicity. *Ironmak. Steelmak.* **2004**, *31*, 125–130. [CrossRef]
11. Mills, K. *The Estimation of Slag Properties*; Southern African Pyrometallurgy: London, UK, 2011; pp. 35–45.
12. Han, C.; Chen, M.; Zhang, W.D.; Zhao, Z.X.; Evans, T.; Nguyen, A.V.; Zhao, B.J. Viscosity model for iron blast furnace slags in SiO_2–Al_2O_3–CaO–MgO system. *Steel Res. Int.* **2015**, *86*, 678–685. [CrossRef]
13. Ji, F.Z.; Du, Z.C.; Seetharaman, S. Viscosities of multicomponent silicate melts at high temperatures. *Int. J. Thermophys.* **1999**, *20*, 309–323. [CrossRef]
14. Iida, T.; Sakai, H.; Kita, Y.; Shigeno, K. An equation for accurate prediction of the viscosities of blast furnace type slags from chemical composition. *ISIJ Int.* **2000**, *40*, 110–114. [CrossRef] [PubMed]
15. Zhang, G.H.; Chou, K.C.; Mills, K. Modelling viscosities of CaO–MgO–Al_2O_3–SiO_2 molten slags. *ISIJ Int.* **2012**, *52*, 355–362. [CrossRef]

16. Guo, H.W.; Zhu, M.Y.; Yan, B.J.; Deng, S.C.; Li, X.Y.; Liu, F. Dynamic regional viscosity prediction model of blast furnace slag based on the partial least-squares regression. *JOM* **2017**, *69*, 395–401. [CrossRef]
17. Jiang, D.W.; Zhang, J.L.; Wang, Z.Y.; Feng, C.F.; Jiao, K.X.; Xu, R.Z. A prediction model of blast furnace slag viscosity based on principal component analysis and k-nearest neighbor regression. *JOM* **2020**, *72*, 3908–3916. [CrossRef]
18. Han, C.; Chen, M.; Zhang, W.D.; Zhao, Z.X.; Evans, T.; Zhao, B.J. Evaluation of existing viscosity data and models and developments of new viscosity model for fully liquid slag in the SiO_2–Al_2O_3–CaO–MgO system. *Metall. Mater. Trans. B* **2016**, *47*, 2861–2874. [CrossRef]
19. Zheng, H.Y.; Ding, Y.Q.; Zhou, S.F.; Wen, Q.L.; Jiang, X.; Gao, Q.J.; Shen, F.M. Viscosity prediction model for blast furnace slag with high Al_2O_3. *Steel Res. Int.* **2021**, *92*, 900635. [CrossRef]
20. Mills, K.C.; Chapman, L.; Fox, A.B.; Sridha, S. "Round robin" project on the estimation of slag viscosities. *Scand. J. Metall.* **2001**, *30*, 396–403. [CrossRef]
21. Zhang, S.; Zhang, X.; Peng, H. Structure analysis of CaO–SiO_2 –Al_2O_3 –TiO_2 slag by molecular dynamics simulation and FTIR spectroscopy. *Trans. Iron Steel Inst. Jpn.* **2014**, *54*, 734–742. [CrossRef]
22. Shankar, A.; Görnerup, M.; Lahiri, A.K.; Seetharaman, S. Experimental investigation of the viscosities in CaO–SiO_2–MgO–Al_2O_3 and CaO–SiO_2–MgO–Al_2O_3–TiO_2 Slags. *Metall. Mater. Trans. B* **2007**, *38*, 911–915. [CrossRef]
23. Datta, K.; Sen, P.K.; Gupta, S.S.; Chatterjee, A. Effect of titania on the characteristics of blast furnace slags. *Steel Res. Int.* **1993**, *64*, 232–238. [CrossRef]
24. Yuan, X.; Zhang, J.L.; Mao, R.; Liu, Z.J.; Zhu, G.Y. Viscosity and Melting Property of Low Titanium-containing Blast Furnace Slag. *J. Process Eng.* **2014**, *04*, 664–670.
25. Park, H.; Park, J.Y.; Kim, G.H.; Sohn, I. Effect of TiO_2 on the viscosity and slag structure in blast furnace type slags. *Steel Res. Int.* **2012**, *83*, 150–156. [CrossRef]
26. Kim, W.H.; Sohn, I.; Min, D.J. A Study on the viscous behaviour with K_2O additions in the CaO–SiO_2–Al_2O_3–MgO–K_2O quinary slag system. *Steel Res. Int.* **2010**, *81*, 735–741. [CrossRef]